Vacuum 130 (2016) 63–71

Contents lists available at ScienceDirect

Vacuum

journal homepage: www.elsevier.com/locate/vacuum

Melt processing and properties of linear low density polyethylene-graphene nanoplatelet composites

P. Noorunnisa Khanam [a], M.A. AlMaadeed [a, b, *], M. Ouederni [c], Eileen Harkin-Jones [d], Beatriz Mayoral [e], Andrew Hamilton [e], Dan Sun [e]

[a] Center for Advanced Materials, Qatar University, 2713, Doha, Qatar
[b] Materials Science and Technology Program, Qatar University, 2713, Doha, Qatar
[c] Qatar Petrochemical Company, Qatar
[d] School of Engineering, University of Ulster, UK
[e] School of Mechanical & Aerospace Engineering, Queen's University Belfast, UK

ARTICLE INFO

Article history:
Received 5 January 2016
Received in revised form
5 March 2016
Accepted 21 April 2016
Available online 22 April 2016

Keywords:
Melt processing
Graphene nanoplatelets
Mechanical properties
Electrical properties

ABSTRACT

Composites of Linear Low Density Polyethylene (LLDPE) and Graphene Nanoplatelets (GNPs) were processed using a twin screw extruder under different extrusion conditions. The effects of screw speed, feeder speed and GNP content on the electrical, thermal and mechanical properties of composites were investigated. The inclusion of GNPs in the matrix improved the thermal stability and conductivity by 2.7% and 43%, respectively. The electrical conductivity improved from 10^{-11} to 10^{-5} S/m at 150 rpm due to the high thermal stability of the GNPs and the formation of phonon and charge carrier networks in the polymer matrix. Higher extruder speeds result in a better distribution of the GNPs in the matrix and a significant increase in thermal stability and thermal conductivity. However, this effect is not significant for the electrical conductivity and tensile strength. The addition of GNPs increased the viscosity of the polymer, which will lead to higher processing power requirements. Increasing the extruder speed led to a reduction in viscosity, which is due to thermal degradation and/or chain scission. Thus, while high speeds result in better dispersions, the speed needs to be optimized to prevent detrimental impacts on the properties.

1. Introduction

Graphene which is a two-dimensional, single-layer of sp2 hybridized carbon atoms, has attracted researchers due to its excellent properties, such as high electrical conductivity, high thermal stability and high mechanical strength. These excellent properties along with its simple manufacture and functionalization makes graphene an ideal to be added in different functional materials. Graphene and graphene based materials have already been used in many applications such as electronic and electrical field [1,2].

Industrial and academic are highly interested in graphene and graphene polymer nano composites [3]. Graphene has a higher surface-to-volume ratio compared to carbon nanotubes (CNTs) as the inner surface of the nanotubes is not accessible to the polymer molecules [4,5], which makes graphene more favorable than CNTs for optimizing the required function or application such as the modification in the electrical, thermal, mechanical and microwave absorption properties. Another advantage is that graphene has lower cost [4–6] choice compared to CNTs because it can be easily made from graphite in large quantities [5]. In the literature, researchers have used various polymers as matrices to prepare the required modified graphene/polymer composites [5], the mechanical, electrical [7–9], thermal [9], and various other properties [10] have been extensively investigated.

Many methods described in literature about the preparation of graphene such as exfoliation of the graphite by micromechanical methods, chemical methods [4,5] or chemical vapor deposition.

Rouff and coworkers [11,12] synthesized graphene from graphite. The reduction of the GO was performed using hydrazine hydrate (chemical method). Single sheets of graphene were prepared via oxidation and thermal expansion of graphite [13]. The synthesis of graphene films with thicknesses of a few layers via CVD was reported by Somani et al. [14], where camphor was used as the precursor on Ni foils. Graphene was prepared via the exfoliation of

* Corresponding author.
E-mail address: m.alali@qu.edu.qa (M.A. AlMaadeed).

http://dx.doi.org/10.1016/j.vacuum.2016.04.022

graphite in aromatic solutions. Grandthys et al. [15] induced the epitaxial growth of graphene on a transition metal using chemical vapor deposition and liquid phase deposition. A high yield of graphene was produced via the liquid-phase exfoliation of graphite [16].

Graphene nanoplatelets (GNPs) are platelet-like graphite nanocrystals containing multiple graphene layers. Maximum stress transfer from the polymer to the filler is achieved with the high interaction zone between the polymer and the filler which can increase the mechanical properties of the composites. Due to the ultra-high aspect ratio (600–10,000), properties of GNPs can have better filler than other fillers in polymer composites. The planar structure of the GNPs provides a 2D path for phonon transport, which provides a large surface contact area with the polymer matrix, which can increase the thermal conductivity of the composite [17]. Common techniques to produce GNPs include chemical reduction of homogeneous colloidal suspension of single layered graphene oxide [18] and by exfoliation of natural graphite flakes by oxidation reaction [19]. Some of researchers prepared GNPs from natural graphite via exfoliation and intercalation with tetra alkyl ammonium bromide [20]. Others such as Cameron Derry et. Al [21]. prepared the GNPs by electric heating acid method.

The aggregation and stacking of graphene nanoplatelets limited the performance of graphene polymer nanocomposites. Because the aggregated GNPs properties can be similar to the graphite with its limited specific surface area. The performance of GNPs can be reduced due to aggregation, which should be addressed as an issue if the potential of GNPs as reinforcing agents is to be realized. Therefore, the objective of this current research is to determine how compounding conditions can influence dispersion and subsequent composite properties.

Linear Low Density Polyethylene (LLDPE) was chosen as the matrix material in this research due to its significant commercial importance. LLDPE has grown most rapidly within the PE (polyethylene) family due to its good balance of mechanical properties and processability compared to other types of PE [22]. Electrically conductive PE based composite materials can be used as electromagnetic-reflective materials, as well as in high voltage cables.

As stated earlier, it is important to achieve good dispersion of a filler material to realize enhancement of the mechanical properties. What is not so clear is how the dispersion state influences the electrical conductivity, and the optimum dispersion state is currently being debated in the literature.

This work attempts to advance knowledge in the area of melt-processed GNP polymer composites by investigating the influence of the compounding conditions on the electrical, thermal and mechanical properties of the GNP/LLDPE composites.

2. Experimental

2.1. Materials

2.1.1. Polymer matrix

LLDPE (MFI = 1 g/cm^3) in powder form was kindly supplied by Qatar Petrochemical Company (QAPCO), Qatar. Prior to the melt processing, 0.4 g of phenolic stabilizer was added for each 1 kg of LLDPE to protect it from degradation during the high temperature processing.

2.1.2. Filler

Graphene nanoplatelets of grade C (C-GNPs) were purchased from XG sciences. Grade C particles have diameter of less than 2 μm. They consist of aggregates of sub-micron platelets. Particle thickness of C-GNPs is 1–5 nm which depends on the surface area. Average Surface area of Grade C particles is 500 m^2/g.

2.2. Preparation of LLDPE/graphene nano composites pellets

LLDPE composites reinforced with 1,2,4,6,8 and 10 wt% 'C' grade graphene were processed using a five-stage Brabender twin screw extruder with three different screw/feeder speeds as shown in Fig. 1. The temperatures of the processing zones were in the range of 190–230 °C. The processing zone temperatures were chosen according to previous reports [23]. Table 1 lists the experimental sets that were executed The polymer/C-GNPs mixtures were fed into the hopper and extruded into strands, which were then cooled in water and granulated into pellets. Fig. 1 shows a schematic diagram of the twin screw extruder. The extruded pellets were subsequently hot pressed into plaques via compression molding. They were held for 20 min in the press at a temperature of 170 °C [24] before a pressure of 165.5 MPa was applied for 20 min. The plaques were then cooled at room temperature. The plaque dimensions were 5 cm length × 5 cm width × 0.5 cm thick.

2.3. Characterizations

2.3.1. Scanning electron microscopy (SEM)

Philips EDX scanning electron microscope (SEM) was used to analyze the morphological analysis. To study the graphene nanoplatelets morphology, 10 mg of the sheets was dispersed in 10 ml of acetone, and the solution was sonicated for 30 min. Cross sections of the composite samples after tensile testing was studied by using SEM which investigate the dispersion of the graphene nanoplatelets in the polymer matrix. SEM was used (3 KV) with high vacuum and different magnifications. The images were collected without coating the samples.

2.3.2. Transmission electron microscopy (TEM)

The C-GNPs were mixed with acetone and sonicated for 30 min. A drop was coated onto a copper grid and placed in a high resolution transmission electron microscope (FEI TECNAI TF 20, 200 kV), which was used to explore the morphology of the GNPs.

2.3.3. Thermal properties

2.3.3.1. Thermogravimetric analysis (TGA). The thermogravimetric analysis (TGA) of the C-GNPs/LLDPE composites was conducted using a Perkin Elmer 6 under a nitrogen atmosphere from ambient temperature to 700 °C at a heating rate of 10 °C/min. The pellets were heated under nitrogen atmosphere.

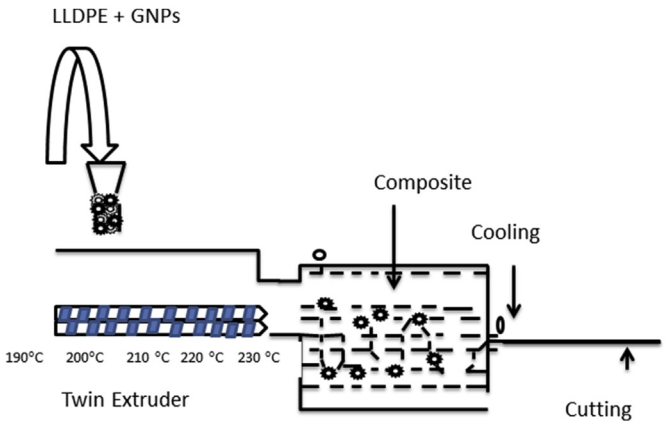

Fig. 1. Schematic diagram of GNPs nanocomposites processing.

Table 1
List of prepared samples with different screw speeds and different feeder speeds.

S.No.	Extruder speed (rpm)	Feeder (kg/h)	% of graphene nanoplateletes	% of LLDPE
1	50	50	0	100
2	100	100	0	100
3	150	150	0	100
4	50	50	1	99
5	50	50	2	98
6	50	50	4	96
7	50	50	6	94
8	50	50	8	92
9	50	50	10	90
10	100	100	1	99
11	100	100	2	98
12	100	100	4	96
13	100	100	6	94
14	100	100	8	92
15	100	100	10	90
16	150	150	1	99
17	150	150	2	98
18	150	150	4	96
19	150	150	6	94
20	150	150	8	92
21	150	150	10	90

2.3.4. Electrical conductivity

A Keithley electrometer (Model 2400) was used to measure the electrical conductivity using the 4 point probe method. Compression molded samples were used in this test. The upper and lower surfaces of the 5 cm × 5 cm plaques were coated with a conducting silver paint to ensure intimate contact between the composite surfaces and electrodes. The electrical conductivity (σ) of the sheet was calculated according to the following formula:

$$\sigma = t/(R_v \times A)$$

where t and A are the thickness of the sheet and effective area of the measuring electrodes, respectively, and R is the resistance of the sample.

2.3.5. Thermal conductivity

The thermal conductivities of the C-GNPs/LLDPE composites were measured using a Hot Disk (Sweden TPS 2500S instrument). The sample dimensions were 5 cm × 2.5 cm with thicknesses of 0.5 cm.

2.3.6. Mechanical testing

The tensile properties of the LLDPE/C-GNPs composites were measured using a universal tensile testing machine at room temperature according to ASTM D638-10. Five samples were tested for each composition, and the average value is reported.

2.3.7. Melt flow index

The melt flow index was measured using a Melt Flow Indexer LMI 4004 machine according to ASTM D1238-10.

3. Results and discussion

3.1. SEM and TEM analysis of graphene nanoplatelets

The morphology of the C-grade graphene nanoplatelets was examined using SEM and TEM at different magnifications. SEM micrographs of the C-GNPs powder are presented in Fig. 2(a), and they show that the C-GNPs were in an agglomerated state.

Graphene nanoplatelets that were sonicated in acetone and dried at room temperature are shown in Fig. 2(b). Multiple graphene sheets in folded or stacked configurations are observed in this image.

Fig. 2(c) shows that the graphene sheets were folded or overlapped. A higher magnification TEM image of a graphene sheet is shown in Fig. 2(d). These elongated sheets can help achieve higher conductivities [25] in the polymer compared to spherical or elliptical fillers because they form a better conducting network.

3.2. Thermal properties

3.2.1. TGA

The TGA results are shown in Fig. 3. The results show the changes in the degradation temperatures across all of the samples. LLDPE begins to degrade at a low temperature, whereas degradation of the graphene nanocomposites is delayed to degrade at higher temperatures due to the protection produced by the graphene in the polymer.

As observed from the curves, the degradation peak temperature increases with increasing filler loading in all cases, suggesting that graphene acts as an effective thermal barrier. The LLDPE nanocomposite with 10 wt% C-GNPs has a higher thermal stability than the rest of the graphene composites. The graphene nanoplatelets prevent the emission of small gaseous molecules, disrupt the oxygen supply during the thermal degradation and cause the formation of charred layers on the surface of the nanocomposite.

Graphene nanoplatelets are likely to act in a similar manner to the addition of nano clays and minerals to polymers [26,27], i.e., causing the formation of charred layers on the surfaces of the composite and disrupting the oxygen supply to the material underneath. Similar results were observed by other researchers in the literature. Graphene increased the thermal stability of PHBR matrices [28] and increased the thermal stability of PP [29]. The thermal stability of PS nanoparticles was improved by the addition of graphene and increased with the graphene content [30].

Increasing the extruder speed increases the degradation temperature, which is likely due to better dispersion of the C-GNPs at the higher shear rate, hence the formation of a better barrier layer.

3.3. Electrical conductivity

The electrical conductivities of the C-GNPs/LLDPE composites are shown in Fig. 4(a). The results show a considerable increase in the electrical conductivity as the C-GNP content increases, which is a confirmation of the impact of addition of the carbon family to

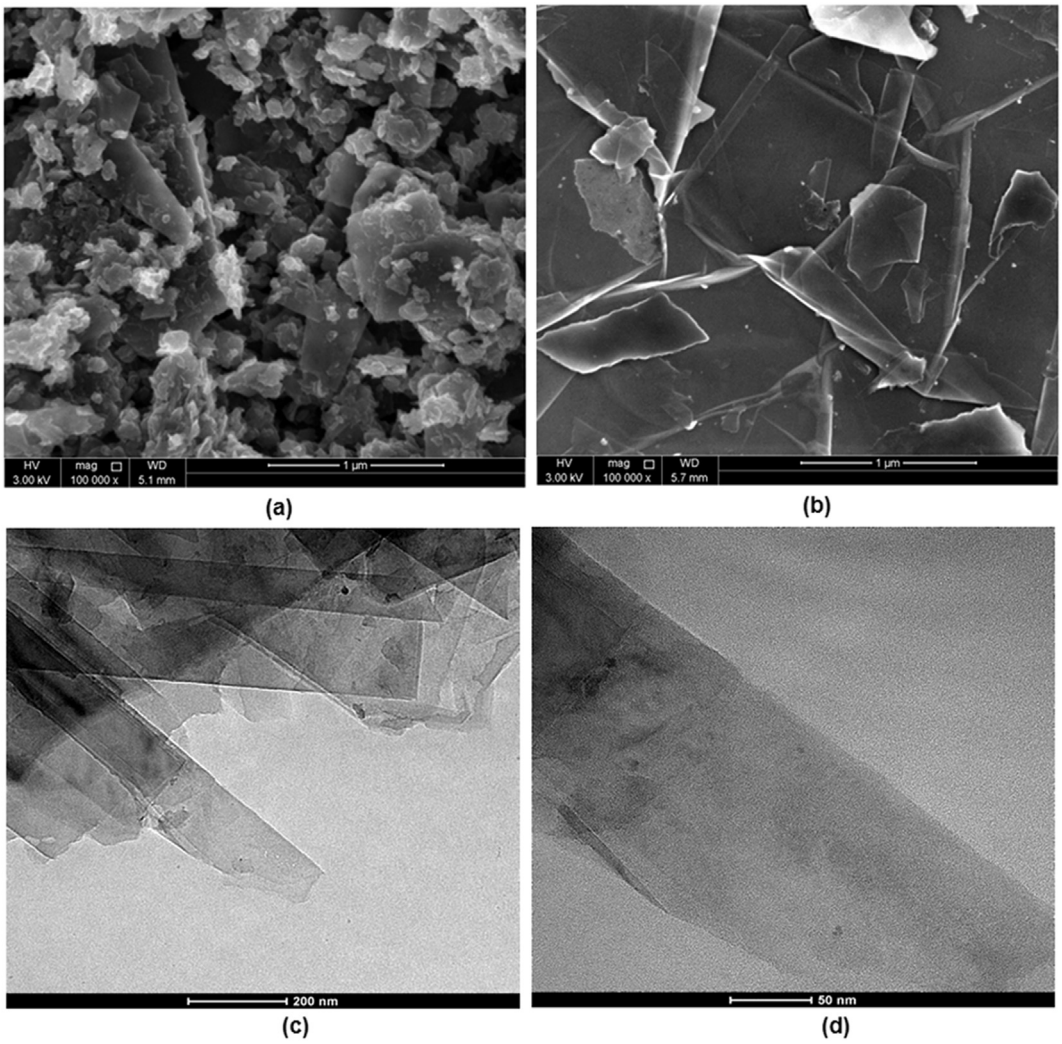

Fig. 2. (a) and (b) SEM images of graphene nanoplatelet powder and (b) sonicated graphene Nanoplatelet (c) and (d) TEM images of graphene nanoplatelet at different magnifications.

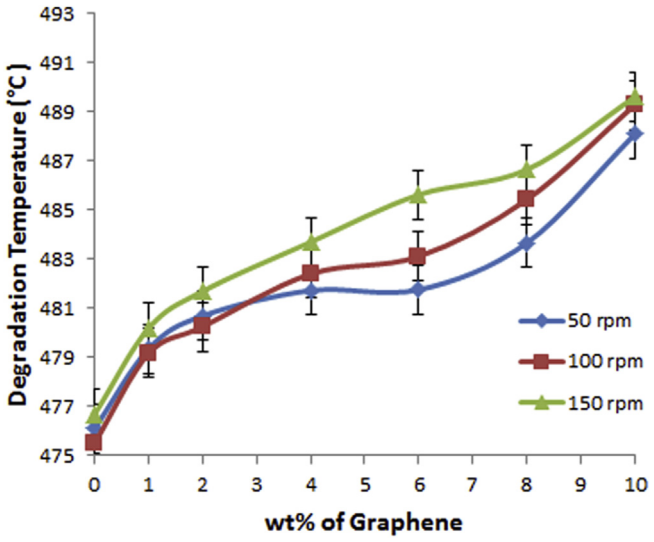

Fig. 3. Effect of C-GNPs addition on the degradation temperature of LLDPE at different extruder/feeder speeds of 50, 100 and 150 rpm.

polymers, as concluded by other studies [28,31]. The electrical conductivity of LLDPE is 2.14×10^{-11} for 50 rpm, 2.81×10^{-11} for 100 rpm and 9.2×10^{-11} for 150 rpm. The high electrical conductivity of the C-GNPs converts the LLDPE insulator to an electrical conductor. Schematic diagram for electrical conducting networks in LLDPE/C-GNPs is shown in Fig. 4(b) which describes the mechanism whereby graphene formed a conductive network in nanocomposites. A. S. Luyt et al. [32] observed the same behavior of increasing conductivity for LLDPE after the addition of copper. The GNPs in the LDPE composites extruded at speeds of 50, 100 and 150 rpm have the following values for the 4% GNP content: 9.36×10^{-08}, 2.9×10^{-08} and 3.94×10^{-07} S/m respectively. As a comparison, a carbon black (CB) content in HDPE of less than 6% [33] results in a value less than 10^{-9} S/m. The conductivity reaches 8.94×0^{-05} for 10% graphene at 150 rpm in our case.

In general, the composites made at 150 rpm exhibit a slightly higher electrical conductivity than those made at 50 and 100 rpm, especially at C-GNP concentrations of greater than 4% in the matrix. This result will be shown later in the SEM photos, which shows that, at 4% filler content, the graphene nanoplatelets have good dispersion compared to other wt% of the C-GNPs composites.

Low concentrations and poor dispersion may lower the conductivity at low wt% of C-GNPs, this is also reported by Kim et al.

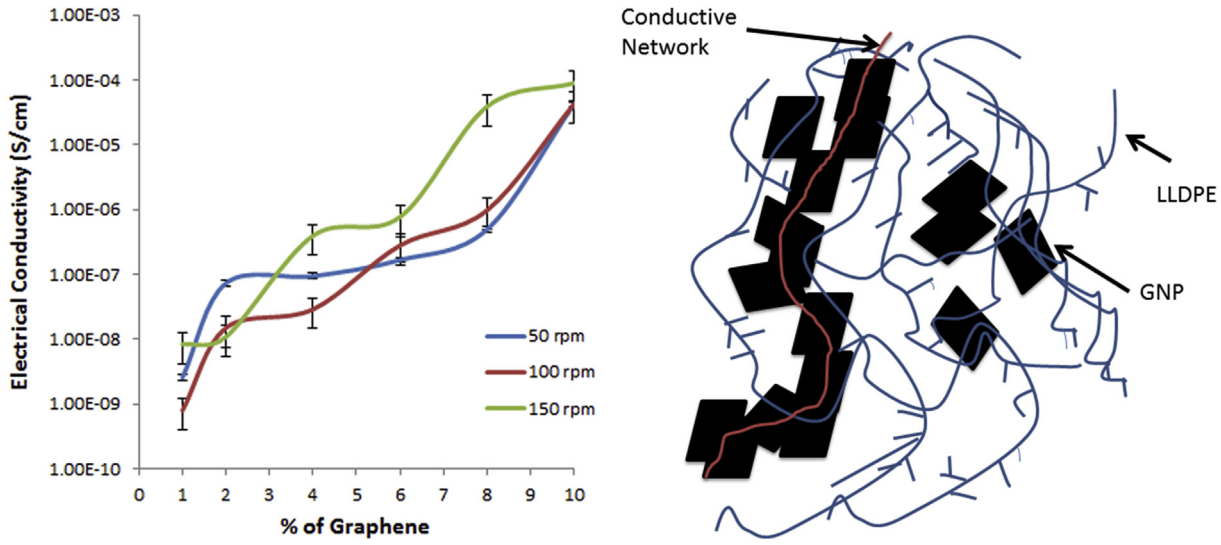

Fig. 4. (a). Effect of C-GNPs addition on the electrical conductivity of LLDPE/C-GNPs composites at different extruder speeds of 50, 100 and 150 rpm, and (b) Schematic diagram of conductive networks formed by C-GNPs in LLDPE/C-GNPs composites.

[22] who showed local enhancement of electrical conductivity due to better dispersion of the graphene and the formation of interconnected network in the material. As the amount of C-GNPs in the polymer increases more electron paths in the composite are created.

The composites made at 150 rpm exhibited better electrical conductivities than the samples made at 50 and 100 rpm. The ANOVA tests (which will be discussed later) showed no significant relationship with the speed, even with the high value achieved at 150 rpm. The increase in the electrical conductivity may be attributed to the restriction of the additives in the amorphous parts of the polymer [32]. Increasing the speed of the extruder results in a lower viscosity of the polymer, as shown by the MFR test, and better dispersion of the C-GNPs. Higher speeds and shear rates are expected to cause more homogeneous distribution of the fillers, which cause good transfer of the electrons.

3.4. Thermal conductivity

The thermal conductivities of the C-GNPs/LLDPE composites are shown in Fig. 5. The presence of crystalline C-GNPs is expected to enhance the heat transfer at the interface between the C-GNPs and the LLDPE [17], the thermal conductivity increased with the addition of the C-GNPs (with the increase in the wt%).

The extruder speed has a pronounced effect on the thermal conductivities of the composites with the highest speed having the greatest positive effect, which is likely due to a better dispersion of the C-GNPs at the higher shear rates. The C-GNPs form a conductive network in the LLDPE matrix, allowing for increased thermal conductivity in the LLDPE. The poor thermal and electrical conductivities inherent to pure LLDPE are enhanced by adding graphene to the polymer in the LLDPE graphene nanocomposites. Filler loading and dispersion in the LLDPE change the thermal conductivity of the polymer composites. In the range between 1 and 4% wt C-GNPs, the thermal conductivity increases slightly because the amount of C-GNPs form a broken system in the LLDPE matrix. Interfacial thermal resistance between the C-GNPs filler and LLDPE matrix are expected at these low percentages of the additives. As the wt% of the C-GNPs in the polymer matrix increases, the thermal conductivity also increases. Thus, the 10 wt% sample has the highest thermal conductivity out of all of the C-GNPs/LLDPE composites.

Graphene fillers, which have high aspect ratios and high surface

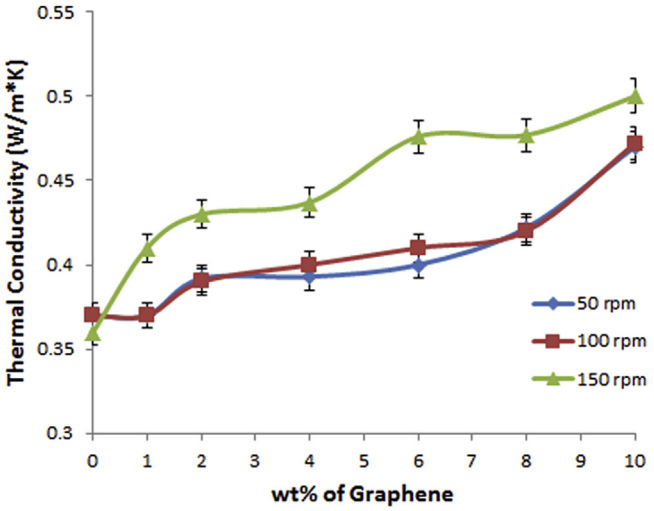

Fig. 5. Effect of graphene % on thermal conductivity of LLDPE/C-GNPs composites at different extruder speeds of 50, 100 and 150 rpm.

area can be arranged in unbroken systems/paths in the polymer matrix and have better enhancement of the thermal transfer [17,34]. Phonons are important factors in the heat conduction of the solid materials. Thermal conductivity of LLDPE/C-GNPs composites was increased because of the phonon conduction mechanism. Generally, adding highly conductive fillers to a polymer increases the thermal conductivity of the composites. Thermal conductivity as well as other thermal properties depend on properties of both the additives and the matrix [17,35]. At low wt%, the fillers in LLDPE are in isolated states. However, when the filler is greater than the percolation threshold of 4 wt%, the fillers aggregate and can arrange unbroken paths for the thermal conductivity. More increase in the wt% of the fillers, can arrange more paths and increase the network [17,36].

3.5. Tensile properties

The tensile strengths of the LLDPE/C-GNPs materials are shown in Fig. 6(a). For the 50 rpm sample, the tensile strength increases by

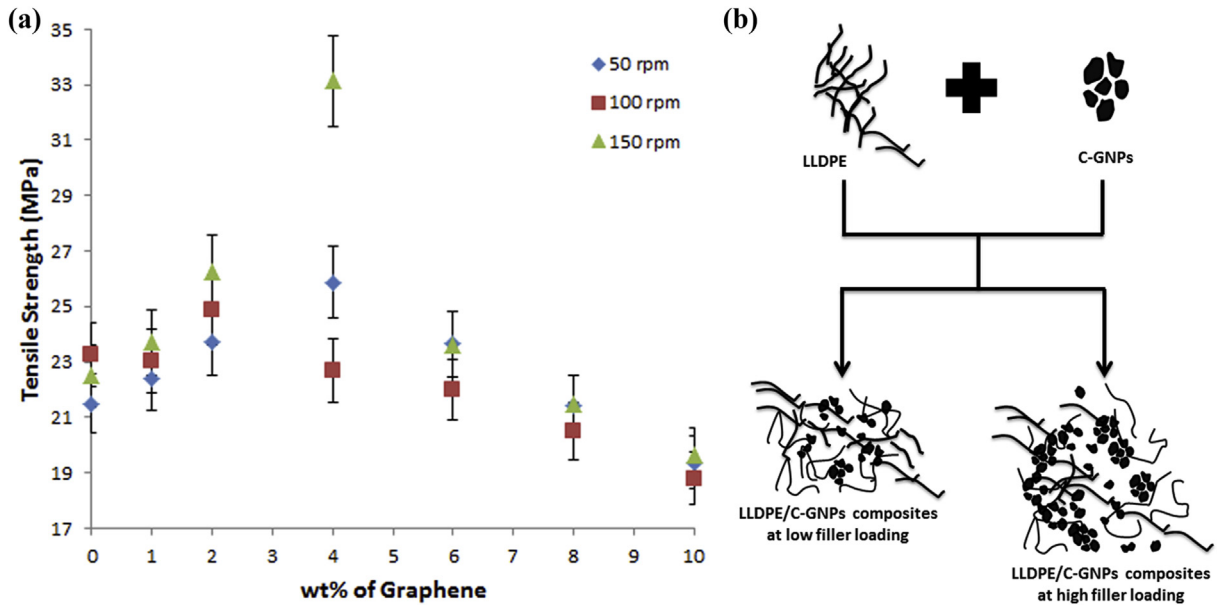

Fig. 6. (a) Effect of graphene addition on tensile strength of LLDPE/C-GNPs composites at different extruder speeds of 50, 100 and 150 rpm and (b) Schematic diagram of LLDPE/C-GNPs composites at low and high wt% of filler.

20.3% at a 4 wt% loading of C-GNPs and then falls off to a value lower than the virgin LLDPE at a loading of 10 wt%. The 100 rpm material increased by 6.8% at 2 wt% loading before falling off to the same level as the 50 rpm material at 10 wt%. At 150 rpm, there is an increase in tensile strength of 47.3% at a loading of 4 wt% C-GNPs.

The tensile strength then falls off dramatically to the same level as the 50 and 100 rpm materials at 10 wt% loading of C-GNPs. The speed effect analyzed using ANOVA (shown in the last part of this paper) showed that there is no significant effect of the speed on the tensile strength even though a published work showed that an enhancement can be achieved in the tensile properties at fast flow and high shear rates [37] due to a decreased residence time.

It appears that the ability of the extruder to break up agglomeration (Fig. 6(b)) is diminished severely at loadings of C-GNPs greater than 4 wt%. The agglomerates act as stress concentrators and reduce the tensile strength. The main reason for the high tensile strength at 4% of C-GNPs loading is the good dispersion and may also be attributed to the possible ordered C-GNPs distribution in the LLDPE matrix. This ordered distribution will be shown in the SEM micrographs.

SEM images (Fig. 7) are used to clarify the reinforcement mechanism and load transfer from the LLDPE to the graphene. Strengthening mechanism of the nano composites was examined by using SEM images which were taken after fracture from tensile test.

The distributions for the lower (e.g., 1% of C-GNPs) and higher (10% of C-GNPs) samples are not well dispersed in the matrix, and agglomeration might occur at high concentrations which is possible due to the Vander Waals force of the nano sheets which are slipped during the tensile testing causing the decrease of mechanical properties of the composites. SEM image of low wt% of filler reinforced composites clearly shown that the strong interface between the graphene and the LLDPE polymer which is an indication that tensile load is effectively transferred from the LLDPE to the graphene and also shows the uniform distribution of graphene [38].

The reader should be careful to not confuse the behavior of the electrical conductivity and the tensile strength because agglomeration cannot affect the electrical conductivity if there is at least one cluster of particles formed in the matrix [32] and the electrons can move throughout the medium in a conductive path. Increasing the filler concentration increases the electrical conducting paths in the matrix [39].

3.6. SEM analysis

The SEM micrographs in Fig. 7 illustrate the shape of the samples after the tensile testing. Fig. 7(a) shows the ductility behavior of the pure LLDPE sample at 150 rpm. All speeds have similar ductility behaviors (not shown).

Adding C-GNPs causes the samples to be more brittle as shown in Fig. 7(b)–(j). The SEM photos show the good distribution of the 4% C-GNPs in the matrix at all speeds. This behavior was confirmed by the higher tensile strength results at this content level. The agglomeration for high wt% for fillers was reported elsewhere [40]. Various published work about the good dispersion of lower wt% of the additives in polymer composites were also reported [39,41,42]. The 1% and 10% C-GNP samples have more brittle behaviors as the samples have less stretched endings [43] compared to 4 wt%. Also the distribution is not perfect with more agglomeration after the addition of 10% C-GNPs.

3.7. Melt flow index

Table 2 shows the melt flow rate (MFR) information for all of the samples. The MFR is inversely proportional to the dynamic viscosity [44]. The MFR decreases with the addition of C-GNPs, which is in agreement with the published literature [45,46], where the incorporation of rigid fillers into a polymer matrix is shown to limit the molecular mobility and increase the material viscosity. Increasing the extruder's speed causes the MFR to increase, which means a decreased molecular weight. This result is likely due to thermal degradation of the polymer and chain scission [47]. The impact of increasing extruder speed on the flow properties of the composite becomes less pronounced as the graphene loading increases because the high additive loading becomes more dominant as a mobility limiting factor than the speed effect.

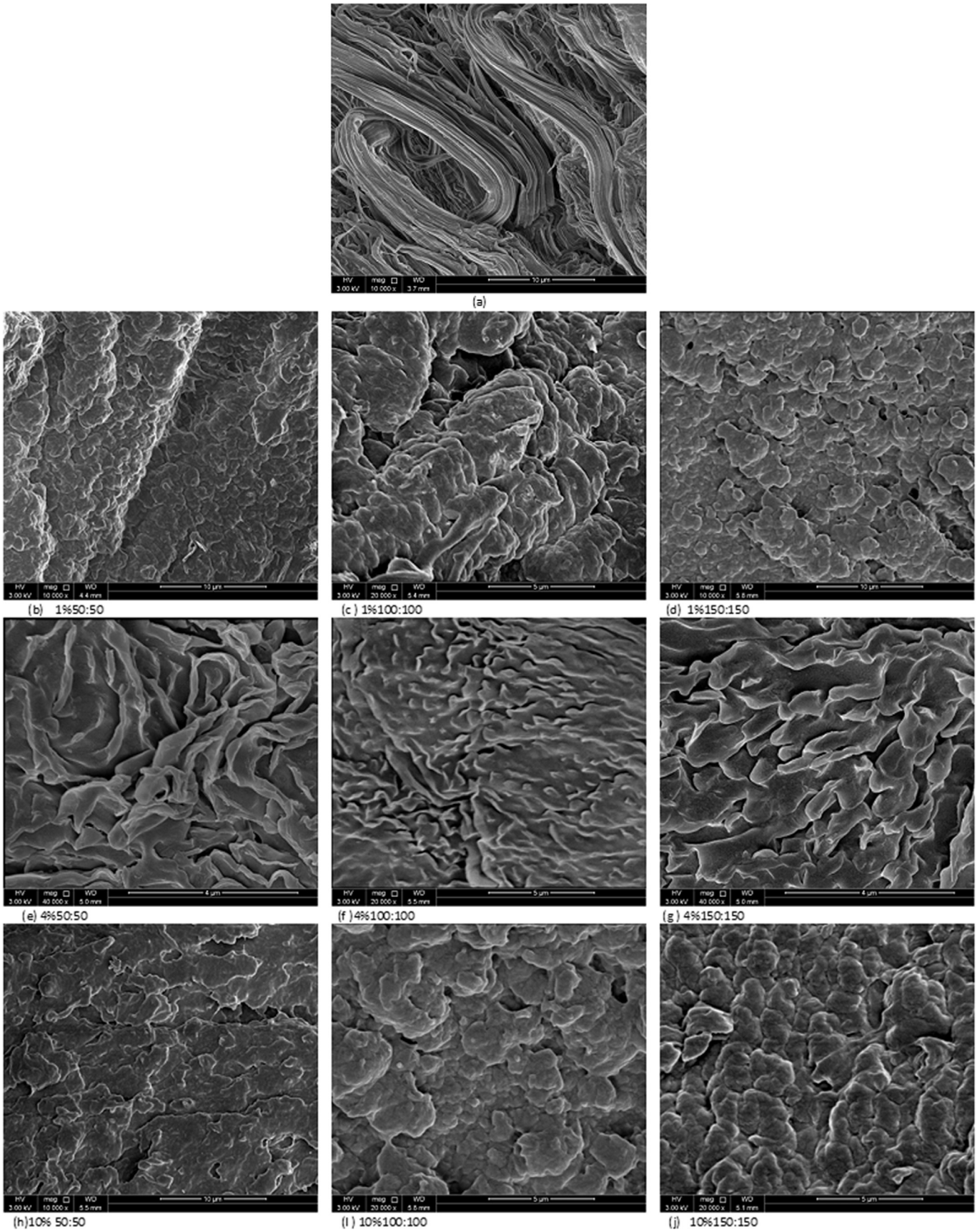

Fig. 7. SEM images of (a) pure LLDPE with 150 rpm speed (b), (c) and (d) corresponds to 1wt% C-GNPs/LLDPE composites at 50,100 and 150 rpm speed respectively; (e), (f) and (g) correspond to 4 wt% of C-GNPs/LLDPE composites at 50,100 and 150 speed respectively; (h), (i) and (j) correspond to 10 wt% of C-GNPs/LLDPE composites at of 50, 100 and 150 rpm respectively.

Table 2
MFR of GNPs/LLDPE composites with different screw speeds.

Samples	MFR for 50 rpm composites (g/10 m)	MFR for 100 rpm composites (g/10 m)	MFR for 150 rpm composites (g/10 m)
LLDPE	0.61	0.79	0.95
1% GNPCs	0.56	0.75	0.91
2%GNPCs	0.54	0.75	0.86
4%GNPCs	0.52	0.67	0.85
6%GNPCs	0.51	0.57	0.83
8%GNPCs	0.50	0.55	0.65
10%GNPCs	0.50	0.52	0.53

Table 3
Two-factor ANOVA without replication on different properties.

Properties	P value (speed)	P value (%of graphene)	F value (speed)	F critical (speed)	F value (%of graphene)	F critical (%of graphene)
Tensile strength	0.13	0.0086	2.36	3.88	5	2.9
Degradation temperature	0.00029	3.4E-10	6.52	3.88	31.78	2.99
Thermal conductivity	0.0019	0.000034	11.04	3.88	16.81	2.99
Electrical conductivity	0.12	0.000462	2.43	3.88	9.9	2.99

Note: F, the F value; P-value, the probability of F value; F-crit, the critical value.

3.8. Analysis of variance (ANOVA)

In this paper, a two factor analysis of variance without replication was used to evaluate the significance of the graphene addition and extruder speed on the properties of the composites. The significance level (α) employed in this investigation is 0.05. The F-tests were performed at a confidence level 95%. The results are shown in Table 3.

The P-values for the degradation temperature, and thermal conductivity are less than the significance level (0.05) for both the graphene percentage and the speed. The F values are greater than F-critical for the same parameters. Therefore, both the speed and the percentage of added graphene are significant for the above properties.

For the effect of graphene addition on the electrical conductivity and tensile strength, the P-values are less than 0.05, and the F-values are greater than F-critical, which suggests that the addition of graphene has a significant effect on these two properties.

For the speed, the P-values for the tensile strength and electrical conductivity are greater than 0.05, and the F-values are smaller than the values of F-critical. This result show that there is no significant relationship between these two properties and the speed of the extruder.

4. Conclusions

The effects of graphene nanoplatelets and extrusion speed on the physical and mechanical properties of LLDPE were studied. Enhancements of the electrical and thermal properties were achieved as the percentage of added C-GNP increased. The thermal conductivity improved significantly at the highest screw speed of 150 rpm, but the speed is not a significant factor in the electrical conductivity. This improved thermal conductivity result is likely due to the better dispersion of the C-GNPs, which results in the formation of more conductive networks. The thermal stability was also enhanced by the addition of the C-GNPs. The tensile strength increased with the addition of C-GNPs up to a loading of 4 wt%. At loadings greater than 4 wt%, even the highest screw speed was unable to break up the agglomerates, which act as stress concentrators and reduce the mechanical performance. The MFR decreased with increasing C-GNP content and decreased with the extruder speed due degradation of the polymer and chain scission.

Acknowledgments

"This work was made possible by NPRP grant No. NPRP5-039-2-014 from the Qatar National Research Fund (A Member of The Qatar Foundation). The statements made herein are solely the responsibility of the authors".

References

[1] X. Huang, Z. Yin, S. Wu, X. Qi, Q. He, Q. Zhang, Q. Yan, F. Boey, H. Zhang, Graphene-based materials: synthesis, characterization, properties and applications, Smal 18 (2011) 1876–1902.
[2] K. Tapan Das, Smita Prusty, Graphene-based polymer composites and their applications, Polym. Plast. Technol. Eng. 52 (4) (2013) 319–331.
[3] Ayesha Kausar, Wajid-Ullah, Bakhtiar Muhammad, Muhammad Siddiq, Influence of processing technique on the physical properties of modified polystyrene/exfoliated graphite nanocomposites, Mater. Manuf. Process 30 (2015) 346–355.
[4] Hu Kesong, D. Dhaval, Ikjun Choi Kulkarni, V. Vladimir, Tsukruk, Graphene-polymer nanocomposites for structural and functional applications, Prog. Polym. Sci. 39 (11) (2014) 1934–1972.
[5] J. Du, H.M. Cheng, The fabrication, properties and uses of graphene/polymer composites, Macro Mol. Chem. Phys. 213 (2012) 1060–1077.
[6] Yiqing Sun, Gaoquan Shi, Graphene/polymer composites for energy applications, J. Polym. Sci. Part B Polym. Phys. 51 (2013) 231–253.
[7] B. Ahmadi-Moghadam, M. Sharafimasooleh, S. Shadlou, F. Taheri, Effect of functionalization of graphene nanoplatelets on the mechanical response of graphene/epoxy composites, Mater. Des. 66 (2015) 142–149.
[8] Pan Ying, Hong Ningning, Zhan Jing, Wang Bibo, Song Lei, Hu Yuan, Effect of graphene on the fire and mechanical performances of glass fiber-reinforced polyamide 6 composites containing aluminum hypophosphite, Polym. Plast. Technol. Eng. 53 (4) (2014) 1467–1475.
[9] F.D.C. Fim, N.R.S. Basso, A.P. Graebin, D.S. Azambuja, G.B. Galland, Thermal, electrical, and mechanical properties of polyethylene-graphene nanocomposites obtained by in situ polymerization, J. Appl. Polym. Sci. 128 (2013) 2630–2637.
[10] Xiaobo Zhu, Tingting Xie, Zunli Mo, Guoping Zho, Chun Zhang, Ruibin Guo, Fabrication of polyaniline/graphene/Tb^{3+} conductive composite, Mater. Manuf. Process 30 (3) (2015) 335–339.
[11] S. Park, R.S. Ruoff, Chemical methods for the production of graphenes, Nat. Nanotechnol. 4 (2009) 217–224.
[12] S. Stankovich, D.A. Dikin, R.D. Piner, K.A. Kohlhaas, A. Kleinhammes, Y. Jia, Y. Wu, S. Nguyen, R.S. Ruoff, Synthesis of graphene-based nanosheets via chemical reduction of exfoliated graphite oxide, Carbon 45 (2007) 1558–1565.
[13] Yupeng Zhang, Delong Li, Xiaojian Tan, Bin Zhang, Xuefeng Ruan, Huijun Liu, Chunxu Pan, Lei Liao, Tianyou Zhai, Yoshio Bando, Shanshan Chen, Weiwei Cai, S. Rodney Ruoff, High quality graphene sheets from graphene oxide by hot-pressing, Carbon 54 (2013) 143–148.
[14] P.R. Somani, S.P. Somani, M. Umeno, Planer nano-graphenes from camphor by CVD, Chem. Phys. Lett. 430 (2006) 56–59.
[15] S. Grandthyll, S. Gsell, M. Weini, M. Schreck, S. Hufner, F. Muller, Epitaxial growth of graphene on transition metal surfaces: chemical vapor deposition versus liquid phase deposition, J. Phys. Condens. Matter 24 (2012) 314204.

[16] Dinh Khoi Dang, Eui Jung Kim, Solvo thermal-assisted liquid-phase exfoliation of graphite in a mixed solvent of toluene and oleylamine, Nanoscale Res. Lett. 10 (2015) 6.
[17] Y. Wang, J. Yu, W. Dai, Y. Song, D. Wang, L. Zeng, N. Jinang, Enhanced thermal and electrical properties of epoxy composites reinforced with graphene nanoplatelets, Polym. Compos. 36 (2015) 556–565.
[18] Y. Geng, S.J. Wang, J.K. Kim, Preparation of graphite nanoplatelets and graphene sheets, J. Colloid Interface Sci. 336 (2009) 592–598.
[19] A.M. Dimiev, G. Ceriotti, A. Metzger, N.D. Kim, J.M. Tour, Chemical mass production of graphene nanoplatelets in ~100% yield, ACS Nano 10 (2016) 274–279.
[20] Q.T. Truong, P. Pokharel, G.S. Song, D.S. Lee, Preparation and characterization of graphene nanoplatelets from natural graphite via intercalation and exfoliation with tetra alkyl ammonium bromide, Nano Sci. Nano Technol. 12 (5) (2012) 4305–4308.
[21] C. Derry, Y. Wu, S. Gardner, S. Zhu, Graphene nanoplatelets prepared by electric heating acid-treated graphite in a vacuum chamber and their use as additives in organic semiconductors, Appl. Mater. Interfaces. 6 (2014) 20269–20275.
[22] H. Kim, S. Kobayashi, M.A. Abdur Rahim, M.J. Zhang, A. Khusainova, M.A. Hillmyer, A.A. Abdala, Graphene/polyethylene nanocomposites: Effect of polyethylene functionalization and blending methods, Polymer 52 (2011) 1837–1846.
[23] M.A. Al Maadeed, M. Ouederni, P. Noorunnisa Khanam, Effect of chain structure on the properties of Glass fibre/polyethylene composites, Mater. Des. 47 (2013) 725–730.
[24] N. Farahbakhsh, P.S. Roodposhti, A. Ayoub, R.A. Venditti, J.S. Jur, Melt extrusion of poly ethylene nanocomposites reinforced with nanofibrillated cellulose from cotton and wood sources, J. Appl. Polym. Sci. 132 (17) (2015), http://dx.doi.org/10.1002/app.41857.
[25] S. Kim, L.T. Drzal, Comparison of exfoliated graphite nanoplatelets (xGnP) and CNTs for reinforcement of EVA nanocomposites fabricated by solution compounding method and three screw rotating systems, J. Adhes. Sci. Technol. 23 (2009) 1623–1638.
[26] Gordon Armstrong, An introduction to polymer nanocomposites, Eur. J. Phys. 2015 (36) (2015) 063001, http://dx.doi.org/10.1088/0143-0807/36/6/063001 (34pp).
[27] S.M. Ardekani, A. Dehghani, M.A. Al Maadeed, M.U. Wahit, A. Hassan, Mechanical and thermal properties of recycled poly(ethylene terephthalate) reinforced newspaper fiber composites, Fibers Polym. 15 (2014) 1531–1538.
[28] V. Sridhar, I. Lee, H.H. Chun, H. Park, Graphene reinforced biodegradable poly (3-hydroxy- butyrate-co-4-hydroxybutyrate) nano composites, eXPRESS Polym. Lett. 7 (2013) 320–328.
[29] Mounir El Achaby, Fatima-Ezzahra Arrakhiz, Sebastien Vaudreuil, Abou el Kacem Qaiss, Mostapha Bousmina, Omar Fassi-Fehri, Mechanical, thermal, and rheological properties of graphene-based polypropylene nanocomposites prepared by melt mixing, Polym. Compos. 33 (5) (2012) 733–744.
[30] Keqing Zhou, Wei Yang, Gang Tang, Bibo Wang, Saihua Jiang, Yuan Hu, Zhou Gui, Comparative study on the thermal stability, flame retardancy and smoke suppression properties of polystyrene composites containing molybdenum disulfide and graphene, RSC Adv. 3 (2013) 25030–25040.
[31] X.Y. Qi, D. Yan, Z. Jiang, Y.K. Cao, Z.Z. Yu, F. Yavari, N. Koratkar, Enhanced electrical conductivity in polystyrene nanocomposites at ultra-low graphene content, ACS Appl. Mater. Interfaces 3 (2011) 3130–3133.
[32] S. Luyt, J.A. Molefi, H. Krump, Thermal, mechanical and electrical properties of copper powder filled low-density and linear low-density polyethylene composites, Polym. Degrad. Stab. 91 (2006) 1629–1636.
[33] A. Markov, B. Fiedler, K. Schulte, Electrical conductivity of carbon black/fibres filled glass-fibre-reinforced thermoplastic composites, Compos. Part A Appl. Sci. Manuf. 37 (2006) 1390–1395.
[34] Jun-Wei Zha, Tian-Xing Zhu, Yun-Hui Wu, Si-Jiao Wang, K.Y. Robert, Lib, Zhi-Min Dang, Tuning of thermal and dielectric properties for epoxy composites filled with electrospun alumina fibers and graphene nanoplatelets through hybridization, J. Mater. Chem. C 3 (2015) 7195–7202.
[35] T. Zhou, X. Wang, P. Cheng, T. Wang, D. Xiong, X. Wang, Improving the thermal conductivity of epoxy resin by the addition of a mixture of graphite nanoplatelets and silicon carbide micro particles, eXPRESS Polym. Lett. 7 (7) (2013) 585–594.
[36] Peng-Gang Ren, Ying-Ying Di, Qian Zhang, Lan Li, Huan Pang, Zhong-Ming Li, Composites of ultrahigh-molecular-weight polyethylene with graphene sheets and/or MWCNTs with segregated network structure: preparation and properties, Macromol. Mater. Eng. 297 (2012) 437–443.
[37] Z.X. Zhang, C. Gao, Z.X. Xina, J.K. Kim, Effects of extruder parameters and silica on physic mechanical and foaming properties of PP/wood-fiber composites, Compos. Part B Eng. 43 (2012) 2047–2057.
[38] D. Lahiri, R. Dua, C. Zhang, I.S. Novoa, A. Bhat, S. Ramaswamy, A. Agarwal, Graphene nanoplatelet induced strengthening of ultra high molecular weight polyethylene and bio-compatibility In Vitro, ACS Appl. Mater. Interfaces 4 (4) (2012) 2234–2241.
[39] Zhen Zhou, Shifeng Wang, Yong Zhang, Yinxi Zhang, Effect of different carbon fillers on the properties of PP composites: comparison of carbon black with multiwalled carbon nanotubes, J. Appl. Polym. Sci. 102 (2006) 4823–4830.
[40] M. Oleksy, K. Szwarc-Rzepka, M. Heneczkowski, R. Oliwa, T. Jesionowski, Epoxy resin composite based on functional hybrid fillers, Materials 7 (8) (2014) 6064–6091.
[41] M.A. AlMaadeed, S. Labidi, Krupa,I, M. Ouederni, Effect of waste wax and chain structure on the mechanical and physical properties of polyethylene, Arabian J. Chem. 8 (2015) 388–399.
[42] P. Noorunnisa Khanam, M.A. Al Maadeed, Processing and characterization of polyethylene-based composites, Adv. Manuf. Polym. Compos. Sci. 1 (2015) 63–79.
[43] Noorunnisa Khanam, M.A. Al-Maadeed, Improvement of ternary recycled polymer blend reinforced with date palm fibre, Mater. Des. 60 (2014) 532–539.
[44] E.E. Ferg, L.L. Bolo, A correlation between the variable melt flow index and the molecular mass distribution of virgin and recycled polypropylene used in the manufacturing of battery cases, Polym. Test. 32 (2013) 1452–1459.
[45] J.Z. Lu, Q. Wu, I.I. Negulescu, Y. Chen, The influences of fiber feature and polymer melt index on mechanical properties of sugarcane fiber/polymer composites, J. Appl. Polym. Sci. 102 (2006) 5607–5619.
[46] Laura Teuber, Holger Militz, Andreas Krause, Processing of wood plastic composites: the influence of feeding method and polymer melt flow rate on particle degradation, J. Appl. Polym. Sci. (2016), http://dx.doi.org/10.1002/APP.43231.
[47] E. Franco-Urquiza, O.O. Santana, J. Gamez-Perez, A.B. Martínez, M. Ll, Maspoch, Influence of processing on the ethylene-vinyl alcohol (EVOH) properties: application of the successive self nucleation and annealing (SSA) technique, eXPRESS Polym. Lett. 4 (3) (2010) 153–160.